

Influence of crosslinking monomer on the formation of copolymer microcapsules encapsulated heat storage material

Priyagorn Pholsrimuang,¹ Piyalak Ngernchuklin,² Amorn Chaiyasat,¹
Preeyaporn Chaiyasat*¹

¹*Department of Chemistry, Faculty of Science and Technology, Rajamangala University of Technology Thanyaburi, Pathumthani 12110, Thailand*

²*Thailand Institute Scientific and Technological Research (TISTR), Pathumthani 12120, Thailand*

*e-mail: p_chaiyasat@mail.rmutt.ac.th

Abstract

In this research, the preparation of methylmethacrylate (MMA)-based copolymer microcapsules to encapsulate Rubitherm27 (RT27) as a heat storage material by microsuspension polymerization was studied. The oil phase consisting of monomer(s), benzoyl peroxide initiator and RT 27 were homogeneously mixed. It was then dispersed in aqueous phase of poly(vinyl alcohol) solution as stabilizer to form oil in water emulsion. The influence of various kinds of crosslinking comonomer, such as ethylene glycol dimethacrylate (EGDMA), trimethylolpropane trimethacrylate (TRIM) and divinylbenzene (DVB), on the formation of microcapsules was investigated. It was found that using hydrophilic crosslinking comonomer as EGDMA and TRIM, nonspherical copolymer microcapsules with low shell strength were obtained. In contrast, using more hydrophobic crosslinking comonomer, like DVB, the spherical P(MMA-DVB) microcapsules with higher microcapsule shell strength were formed. Moreover, the amount of free polymer particles formed in aqueous medium decreased with the increase of the hydrophobicity of crosslinking comonomer.

1. Introduction

Recently, the study of phase change materials (PCMs) or heat storage materials and their applications for thermal energy storage has been an area of extensive research¹. Heat storage or PCMs are attractive for many industrial applications such as air condition of building,^{1,2} solar heat storage,³ thermal adaptable fibers and temperature-adaptable greenhouses textiles and fabrics for clothing.⁴ Among of PCMs, paraffin wax is one of the most attractive materials because of its wide range of melting and crystallization temperatures. Paraffin wax has moderate energy capacity, nontoxic, non-corrosive and also chemically inert.⁵ However, its thermal conductivity is low which limits for the applications. To overcome this drawback, a large surface area is required. Therefore, in recent years,

the encapsulation of paraffin wax has been greatly developed to provide large heat transfer area. Moreover, it also controls the volume change of the storage materials as phase changes occurs and protect the influence from the outside environment⁴. Microencapsulation of PCMs was carried out mainly by suspension polymerization.⁶ However, most of the research works have not focused on the influence of the polymer shell on the thermal properties of the encapsulated paraffin wax. In our previous articles, we have successfully prepared polydivinyl benzene (PDVB) microcapsules with encapsulated hexadecane and octadecane by microsuspension polymerization utilizing a self-assembly Phase Separated Polymer (SaPSeP) method.⁷ The spherical microcapsules with high shell strength were formed. However, it was found that

the latent heats, heats of melting and crystallization, of the encapsulated waxes in the microcapsule were always considerably lower than those of pure waxes. It may be due to incomplete phase separation of the PDVB shell and the wax core. To solve this problem, more hydrophilic polymer shell was used to enhance phase separation. The hydrophilic PMMA microcapsules encapsulated Rubitherm 27 (RT27) was prepared by microsuspension polymerization.⁸ The latent heats of the encapsulated RT27 were high closed to those of pure RT27. However, the microcapsules were nonspherical with multiple dents at the surface. Moreover, large amount of free PMMA particles were observed in an aqueous medium resulting in low capsule shell strength.

Therefore, in this research, the copolymerization of MMA with crosslink monomer to improve the microcapsule shell strength was studied. The influence of various kinds of cross-linking monomer as divinylbenzene (DVB), ethylene glycol dimethacrylate (EGDMA) and trimethylolpropane trimethacrylate (TRIM) on the formation of copolymer microcapsule and their thermal properties were investigated.

2. Materials and Methods

2.1 Materials

MMA (Aldrich, Wisconsin, USA; purity, 99%), EGDMA (Aldrich, Wisconsin, USA; purity, 99%) and TRIM (Aldrich, Wisconsin, USA; purity, 99%) were purified by passing through a column packed with basic aluminium oxide. DVB (Aldrich, Wisconsin, USA; purity, 80%) was washed with 1 M sodium hydroxide (NaOH; BDH Prolabo, Leuven, Belgium) solution to remove the polymerization inhibitors before use. RT27 (Rubitherm Technologies GmbH, Berlin, Germany; Commercial grade) was used as received. Reagent-grade benzoyl peroxide (BPO; Merck, Munich, Germany) was purified by recrystallization. Poly(vinyl alcohol) (PVA; Aldrich, Wisconsin, USA; degree

of saponification 87–90% molecular weight $3\text{--}7 \times 10^4 \text{ g mol}^{-1}$) was used as received.

2.2 Microcapsule preparation

MMA-based copolymer microcapsules encapsulated RT27 were prepared by conventional radical microsuspension polymerization (microsuspension CRP) under the conditions listed in Table 1. Firstly, monomer (s), RT27 and BPO (8 wt% relative to monomer) were homogeneous mixed as an oil phase. It was then poured into a PVA aqueous solution (1 wt%) and homogenized at 5,000 rpm for 5 min to form an oil-in-water emulsion. Secondly, the obtained emulsion was subsequently transferred to a round bottom flask, sealed with a silicone rubber septum and purged with a vacuum- N_2 cycle for five times. It was finally polymerized at 80 °C for 8 h at a stirring rate of 200 rpm.

2.3 Characterization

The prepared microcapsules were observed with an optical microscope (OM, SK-100EB&SK-100ET, Seek Inter Co. Ltd, Thailand) and scanning electron microscope (SEM, JSM-6510, JEOL, JEOL Ltd, Japan) to investigate the inner structure of the microcapsules and the morphology of the surface, respectively. For SEM observations, a small amount of dried microcapsules were placed on a nickel SEM stub and coated with Au. Number- (d_n) and weight (d_w) average diameters of free polymer particles were measured by dynamic light scattering (DLS). For the measurement of the thermal properties, free polymer particles were first removed from each dispersion. The microcapsules were then washed with 2-propanol for 60 seconds to remove unencapsulated wax and impurities⁸ before dried in vacuum oven. The RT27 content in the dried microcapsules was determined by a thermogravimetric analyzer (TGA, TGA 4000, Perkin-Elmer, USA) at a heating rate of 10 °C min^{-1} . The latent heats (ΔH_m and ΔH_c) and the

crystallization (T_c) and melting (T_m) temperatures of the encapsulated RT27 in dried microcapsules after washing were measured with a differential scanning calorimeter (DSC, DSC 4000, Perkin-Elmer, USA) under a N_2 flow in a scanning temperature range of -10 to 40 °C and at heating/cooling rate of 5 °C min^{-1} . To compare the latent heats of the encapsulated RT27 in the washed microcapsules containing different amounts of RT27, ΔH_m and ΔH_c values were given in unit of joules per 1 g of encapsulated RT27 (J/g-RT27). These values were calculated using the following equation from the heating/cooling peak areas of the DSC thermogram and the RT 27 content in each washed microcapsule obtained from the TGA analysis.

Table 1. Reagent amount for the preparation of P(MMA-EGDMA)/RT27, P(MMA-TRIM)/RT27 and P(MMA-DVB)/RT27 microcapsules by micro-suspension CRP^a of comonomer/RT27 droplets^b (monomer/RT27 = 50/50 w/w).

Ingredients	MMA:Crosslink monomer		
	0:100	50:50	100:0
MMA (g)	-	1.25	2.50
Crosslink monomer ^c (g)	2.50	1.25	-
RT 27 (g)	2.50	2.50	2.50
BPO (g)	0.20	0.20	0.20
PVA aqueous solution (1wt%) (g)	45.00	45.00	45.00

^a80 °C, 8 h

^bHomogenized at 5,000 rpm for 5 min

^cEGDMA, TRIM or DVB

$$A = [B/C] \times 100 \quad (1)$$

Where

A = ΔH_m and ΔH_c of the encapsulated RT27 in unit of joules per 1 g of encapsulated RT27 (J/g-RT27)

B = ΔH_m and ΔH_c of the encapsulated RT27 in unit of joules per 1 g (J/g-capsule) obtained from the DSC thermogram

C = % loading (experiment) of RT27 in the washed microcapsules obtained from the TGA thermogram

3. Results & Discussion

3.1 Microcapsules formation

Oil droplets consisting of monomer, RT27 and BPO were dispersed in a PVA aqueous solution. When the polymerization proceeded, polymer molecules reached critical chain length precipitated in the oil phase, resulting in phase separation therein. The polymer molecules were moved to the oil droplet interface because of their higher hydrophilicity and formed a capsule shell with an encapsulated RT27 core. Figure 1 shows the optical and SEM micrographs of the prepared polymer microcapsules containing RT27 with various polymer shells. In the cases of PMMA microcapsules (Figure 1a), low strength polymer microcapsule shell with multidentents on their surfaces was observed. The shell strength was then improved with crosslinked copolymer. Increasing of hydrophobic crosslink polymer as P(MMA-DVB) microcapsules (Figure 2b) represented the spherical microcapsules with a dimple. Using more hydrophilic crosslink polymer as in the case of P(MMA-EGDMA) (Figure 2c), non-spherical microcapsules having lower shell strength were obtained. However, high shell strength of P(MMA-EGDMA) and PMMA compared to P(MMA-TRIM) shell (Figure 2d) was obtained even though the multidentents at the surface still were observed. When the temperature was decreased from polymerization to room temperature, the density of encapsulated RT27 increased leading to the formation of space in microcapsules. If the capsule shell strength was not enough to withstand the external pressure, as a result, the dimple was formed at the surface.^{7e} From these results, EGDMA was not appropriate for use as comonomer which was not further studied.

The suspension states were shown in Figure 2. After centrifuged at 5,000 rpm for 10 min, most of microcapsules floated on the top of suspension due to their lower total density than that of water. The bottom

layer was more turbid in the case of P(MMA-TRIM) than P(MMA-DVB). Moreover, free polymer particles were formed in aqueous medium by emulsion polymerization resulting in the reduction of microcapsule shell strength.⁸ The number-average diameter was in the range of 50-500 nm corresponding with polymer particles prepared by emulsion polymerization. It was found that the amount of free polymer particles of P(MMA-TRIM) (33 %wt related to monomer) was higher than that of P(MMA-DVB) (12 %wt related to monomer) due to their water solubilities (2.01 and 0.0052 g/100 ml for TRIM and DVB, respectively).

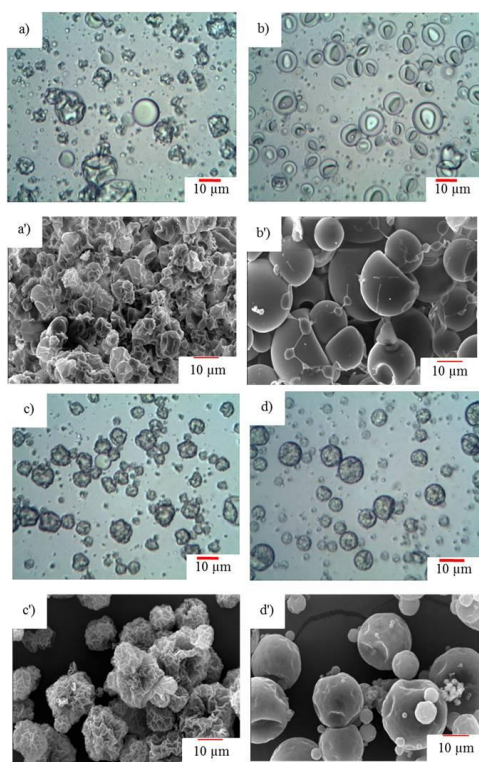


Figure 1. Optical (a, b, c, d) and SEM (a', b', c', d') micrographs of PMMA/RT27 (a, a'), P(MMA-DVB)/RT27 (b, b'), P(MMA-EGDMA)/RT27 (c, c') and P(MMA-TRIM)/RT27 (d, d') microcapsules prepared by microsuspension CRP.

The DSC thermograms of pure RT27 and encapsulate RT27 in various microcapsules are shown in Figure 4. T_m of the encapsulated RT27 in all copolymer microcapsules were about 24 °C similar

with that of pure RT27 (25 °C). In the case of crystallization, the initial T_c values of the encapsulated RT27 were 25 °C closed to that of pure RT 27 (25 °C). However, several small cooling peaks at lower temperature were observed in all cases called supercooling. It may be due to effect of copolymer microcapsules size. The occurrence of supercooling was general phenomena in dispersion system. The impurities located in each micro- capsule could not induce the crystallization and nucleation of RT27 encapsulated in the other microcapsules. Therefore, in the dispersion system, the multiple cooling peaks of RT27 might be based on the different amounts of the impurities in each capsule leading to different nucleation mechanism of both homogeneous and heterogeneous nucleations.⁹

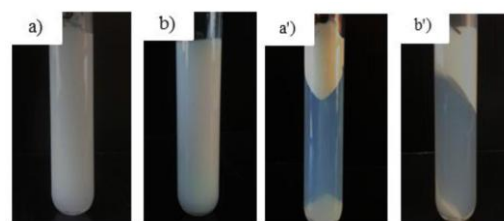


Figure 2. Photos of suspensions before (a and b) and after (a' and b') centrifuged at 5,000 rpm for 10 min of P(MMA-DVB)/RT27 (a), and P(MMA-TRIM)/RT27 (b) microcapsules prepared by micro- suspension CRP.

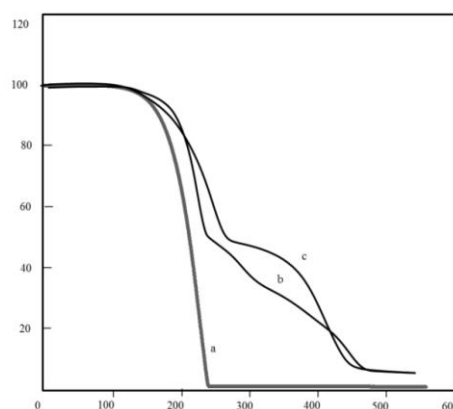


Figure 3. TGA thermograms of pure RT27 (a), P(MMA-TRIM)/RT27 (b) and P(MMA-DVB)/RT27 (c).

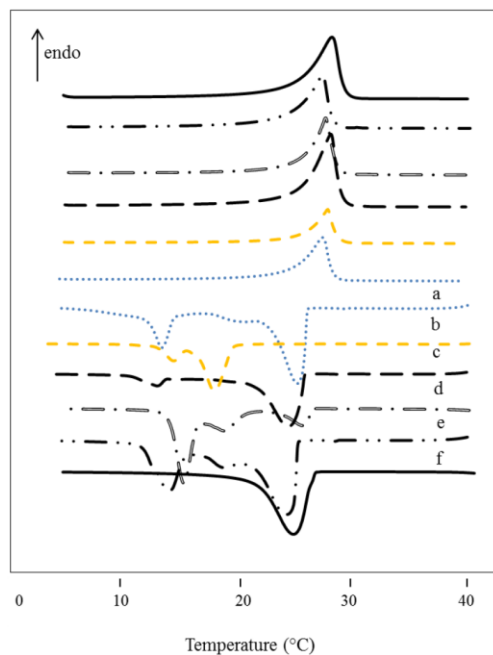


Figure 4. DSC thermograms of encapsulated RT27 in PMMA (a), PDVB (b), PTRIM (c), P(MMA-TRIM)/RT27 (d), P(MMA-DVB)/RT27 (e) microcapsules after removing free particles and washing with 2-propanol and pure RT27 (f).

Table 2. Latent heats of encapsulated RT27 in various copolymer microcapsules prepared by microsuspension CRP.

Copolymer/RT27	Latent heats	
	ΔH_m (J/g-RT27)	ΔH_c (J/g-RT27)
PMMA ^a	164	167
P(MMA-DVB)	134	136
PDVB ^b	127	133
P(MMA-TRIM)	163	167
PTRIM	161	161
RT 27	162	168

^a the data obtained from the Ref. 8

^b the data obtained from the Ref. 9

Table 2 shows the latent heats of encapsulated RT27 in various microcapsules calculated using equation (1). In the case of hydrophobic crosslinked comonomer as PDVB and P(MMA-DVB), lower latent heats than that of pure RT27 were obtained. Using higher hydrophilic shell as PMMA and P(MMA-TRIM), latent heats were increased and closed to that of pure RT27. The increase of

hydrophilicity of polymer shell enhanced phase separation of RT27 core and microcapsule shell. These results well accorded with the results of the P(DVB-acrylate)/HD.^{7e}

4. Conclusions

The MMA-based copolymer microcapsules encapsulated RT 27 were successfully prepared by microsuspension CRP. Using hydrophobic crosslinked comonomer as DVB, spherical microcapsules with high shell strength and low amount of free polymer particles in aqueous medium were formed. However, latent heats of encapsulated RT27 were lower than that of pure RT27. In contrast, the utilization of hydrophilic crosslinked comonomer as TRIM increased the latent heats of encapsulated RT27 in P(MMA-TRIM) microcapsules and those values were closed to that of pure RT27. Nevertheless, non-spherical copolymer microcapsules with lower shell strength were obtained with large amount of free polymer particle.

Acknowledgements

This work was partially supported by The National Research Council, Thailand (No. 182674; given to P.C. and A.C.) and Thailand Institute of Scientific and Technological Research (given to P. P.).

References

1. Agyenim, F.; Hewitt, N.; Eames, P.; Smyth, M. A. *Renewable Sustainable Energy Rev.* **2010**, *14*, 615–628.
2. Zhu, N.; Ma, Z.; Wang, S. *Energy Convers. Manage.* **2009**, *50*, 3169–3181.
3. Qiu, X.; Song, G.; Chu, X.; Li, X.; Tang, G. *Sol. Energy* **2013**, *91*, 212–220.
4. (a) Sánchez-Silva, L.; Rodríguez, J. F.; Romero, A.; Sánchez, P. *J. Appl. Polym. Sci.* **2012**, *124*, 4809–4818; (b)

- Azizi, N.; Ladhari, N.; Majdoub, M. *Asian J. Text* **2011**, *1*, 130–137.
5. Sharma, A.; Tyagi, V. V.; Chen, C. R.; Buddhi, D. *Renew. Sust. Energy Rev.* **2009**, *13*, 318–345.
6. (a) Al-Shannaq, R.; Kurdi, J.; Al-Muhtaseb, S.; Dickinson, M.; Farid, M. *Energy* **2015**, *87*, 654–662; (b) Tang, X.; Li, W.; Zhang, X.; Shi, H. *Energy* **2014**, *68*, 160–166; (c) Tang, X.; Li, W.; Shi, H.; Wang, J.; Han, N.; Zhang, X. *Sci. Adv. Mater.* **2014**, *6*, 120–127; (d) Ma, Y.; Sun, S.; Li, J.; Tang, G. *Thermochim. Acta* **2014**, *588*, 38–46.
7. (a) Chaiyasat, P.; Islam, M. Z.; Chaiyasat, A. *RSC Adv.* **2013**, *3*, 10202–10207; (b) Supatimusro, D.; Promdsorn, S.; Thipsit, S.; Boontung, W.; Chaiyasat, P.; Chaiyasat, A. *Polym. Plast. Technol. Eng.* **2012**, *51*, 1167–1172; (c) Chaiyasat, A.; Waree, C.; Songkhamrod, K.; Sirithip, P.; Voranuch, V.; Chaiyasat, P. *Express Polym. Lett.* **2012**, *6*, 70–77; (d) Chaiyasat, P.; Chaiyasat, A.; Boontung, W.; Promdsorn, S.; Thipsit, S. *Mater. Sci. Appl.* **2011**, *2*, 1007–1013; (e) Chaiyasat, P.; Ogino, Y.; Suzuki, T.; Minami, H.; Okubo, M. *Colloid Polym. Sci.* **2008**, *286*, 217–223.
8. Chaiyasat, P.; Noppalit, S.; Okubo, M.; Chaiyasat, A. *Phys. Chem. Chem. Phys.* **2015**, *17*, 1053–1059.
9. Cao, F.; Yang, B. *Appl. Energ* **2014**, *113*, 1512–1518.